

Unified treatment of the $pd \rightarrow dp$ and $pp \rightarrow \pi^+ d$ processes in a model of N and N^* exchanges

J. S. Sharma and A. N. Mitra

Department of Physics and Astrophysics, University of Delhi, Delhi-110007, India

(Received 28 February 1973; revised manuscript received 15 May 1973)

We present a unified account of two related processes, $pd \rightarrow dp$ and $pp \rightarrow \pi^+ d$, in a scheme of higher baryon couplings developed by this group. The work which represents a considerably improved version of an earlier model for the study of the $pd \rightarrow dp$ process at moderately high energies (1.0–1.5 GeV) is now extended to include (i) lower energies (down to 300 MeV) for $pd \rightarrow dp$, and (ii) the related process $pp \rightarrow \pi^+ d$, within a common set of assumptions for the N and N^* exchange vertices. The fits to the data for both the processes come out rather well over their respective energy ranges, which are appreciable.

I. INTRODUCTION

The two related processes of $pp \rightarrow \pi^+ d$ and $pd \rightarrow dp$ have been the subject of much study, especially over the last half decade, in order to provide an insight into their main experimental features which constitute (i) a fairly sharp drop of the differential cross section with angle away from the backward direction and (ii) a steep fall with energy at backward angles.¹⁻⁸ The obvious mechanism of one-nucleon exchange which offers a simple understanding of the sharp drop in the u variable in terms of the deuteron's form factor does not, unfortunately, generate an adequate magnitude for the cross sections. A second mechanism, first proposed by Yao,⁹ and investigated in considerable detail by Craigie and Wilkin,¹⁰ is the so-called triangle (or pion-exchange) diagram, which brings out rather clearly the similarity of features exhibited by these two processes. In particular the variations with energy and angle are reproduced reasonably well, though the absolute magnitude of the cross sections remains rather low. However, the Yao approximation has recently been criticized and improved upon by Kolybasov and Smorodinskaya,¹¹ who discovered some major integration errors in the former. A somewhat different, perhaps more promising, mechanism to augment the absolute magnitudes of the cross sections was suggested by Kerman and Kisslinger,¹² who proposed the inclusion of at least the $N^*(1688)$ of $J^P = \frac{5}{2}^+$ through a Reggeized N -exchange mechanism. This model was criticized by CW¹⁰ on the grounds that Reggeization at an energy of around 1.0 GeV, where the rest masses themselves involved are of a similar magnitude, is probably too optimistic, yet it is probably fair to say that subject to suitable modifications of the details, the basic KK proposal¹² on the role of resonances for such processes represents an important

physical step in the understanding of these processes in the intermediate energy region, where the window naturally opens up to the "resonances." We record for the sake of completeness that, as pointed out by CW, the failure of the impulse approximation for these processes, even with Glauber corrections to higher orders,¹³ stems from a basic lack of ingredients in such a mechanism to simulate an intrinsically "backward" process.

Some time ago we studied in some detail the effect of N^* exchanges (in addition to N exchange) on the process¹⁴ $pd \rightarrow dp$ through a fairly elaborate model of higher baryon couplings,^{15,16} which has by now been applied quite successfully to several two-body processes up to moderate energies.^{17,18} In this model both the shapes and magnitudes of the $pd \rightarrow dp$ process could be accounted for collectively in terms of a set of several N^* resonances, though each individual resonance plays only a modest role. However, this calculation suffered from the inadequacy of the Yao approximation⁹ subsequently pointed out by KS.¹¹ One adverse result of this defect turned out to be that the angular distributions had shown distortions away from the backward direction for incident energies upwards of 1.3 GeV (Ref. 14) because of the increasingly important role of the high-spin N^* exchanges (like $N^*(1688)$ beyond 1.0 GeV. On the other hand, this calculation, which made a systematic survey of the effects of an entire list of resonances of masses ranging from 1.0 to 2.0 GeV, brought out rather clearly the dominance of $J = L + \frac{1}{2}$ states (L representing the total quantum orbital excitation) over $J = L - \frac{1}{2}$ states, which will not therefore be considered further in this paper.

In this paper we wish to present a unified account of the $pd \rightarrow dp$ and $pp \rightarrow \pi^+ d$ processes within the same model of higher baryon couplings, which has since been refined in certain respects. The basic

mechanism for the evaluation of the dNN^* vertex is the same as described in SBM, but we now have (i) taken advantage of the improvement suggested by KS¹¹ over the Yao approximation⁹ and (ii) made some refinements over Ref. 14 with respect to the coupling structure as well as the form factors (to be defined in Sec. II), in conformity with more recent calculations of certain two-body processes up to moderately high energies.¹⁸ Since both these processes are similar, the pattern of calculations will be described in a common fashion as far as possible.

In Sec. II we summarize the structures of the $pd-dp$ and $pp-\pi^+d$ amplitudes corresponding to the N -exchange diagram. The $NN\pi$ and $N^*N\pi$ coupling structures are also given in Sec. II. In Sec. III the necessary details for the evaluation of the dNN^* vertices and calculation of percentage probabilities of various N^* 's in deuteron are given. The results obtained by this model for the process $pd-dp$ are discussed in Sec. IV in relation to experiment. The discussion of numerical values of probability densities is also presented in Sec. IV. In Sec. V the evaluation of the $pp-\pi^+d$ cross section taking account of the N and N^* exchanges (together with their interference effects) is given. The results of our calculation for the processes $pp-\pi^+d$ are also described in Sec. V in relation to the experimental data. Finally, Sec. VI summarizes our main conclusions.

II. BASIC INGREDIENTS OF THE MODEL

In this section we summarize, for the sake of a self-contained presentation, the essential ingredients for the evaluation of the amplitudes of the two processes. While the general method follows the pattern of Ref. 14, there are a few differences in detail, and in particular certain items of Ref. 14 which have become redundant will be omitted.

A. The extended dNN form factor

Unlike Ref. 14, where the point dNN vertex was used for the calculation of dNN^* couplings via the triangle diagram, we shall now use only the extended dNN form factor for both the dNN and dNN^* couplings [Figs. 1(a) and 1(c)]. In the notation of SBM, but written in a slightly different normalization convention, the dNN form factor^{19, 20} is given by

$$\Gamma(d, P)C = \frac{4\pi}{m} \bar{N}_y \frac{m_a - i\gamma \cdot d}{2\sqrt{2}m_a} \left\{ (\gamma \cdot \epsilon) \left[C(\vec{k}^2) + \frac{m^2 - u}{2\sqrt{2}} \bar{T}(\vec{k}^2) \right] - \frac{3}{\sqrt{2}} \bar{T}(\vec{k}^2) \vec{k} \cdot \epsilon \vec{k} \cdot \gamma \right\} C, \quad (2.1)$$

where the proton, deuteron, and the exchanged-nucleon momentum 4-vectors are \not{p}_μ , \not{d}_μ , and \not{P}_μ , respectively, and ϵ_μ is the deuteron polarization 4-vector;

$$\vec{k}_\mu = \frac{1}{2}(\not{p}_\mu - \not{P}_\mu), \quad \not{d}_\mu = \not{p}_\mu + \not{P}_\mu, \quad (2.2)$$

$$d \cdot \vec{k} = d \cdot \epsilon = 0, \quad (2.3)$$

$$\vec{k}^2 = \vec{k}_\mu \vec{k}_\mu = -\alpha^2 + \frac{1}{2}(m^2 - u), \quad P^2 = -u, \quad (2.4)$$

$$(\bar{N}_y)^{-2} = (2\pi^2) \int d\vec{q} g^2(\vec{q}) (\vec{q}^2 + \alpha^2)^{-2}, \quad (2.5)$$

$$g(\vec{k}^2) = C(\vec{k}^2) - \frac{1}{2} \vec{\sigma} \cdot \vec{k} \vec{\epsilon} \cdot \vec{k} \bar{T}(\vec{k}^2), \quad (2.6)$$

$$C = i\gamma_4 \gamma_2, \quad C\gamma_\mu^T C^{-1} = -\gamma_\mu, \quad C\gamma_5^T C^{-1} = +\gamma_5. \quad (2.7)$$

B. The $NN\pi$ and $NN^*\pi$ couplings

The $NN\pi$ coupling will be needed for two types of evaluation: (i) $pp-\pi^+d$ amplitude via N exchange and (ii) the triangular dNN^* vertex [Fig. 1(c)]. The $N^*N\pi$ coupling [Fig. 1(b)] will be required at the corresponding places when the exchange nucleon is substituted by an N^* . For the N^* 's, of which

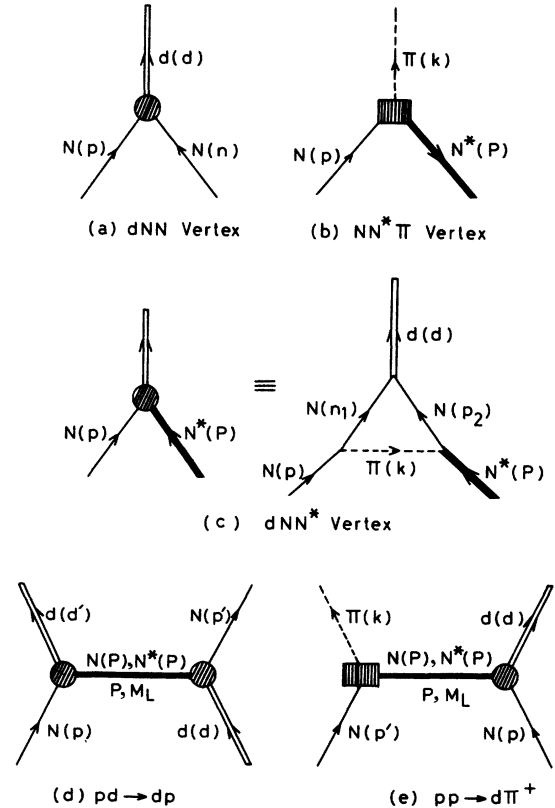


FIG. 1. (a) dNN vertex, (b) $NN^*\pi$ vertex, (c) dNN^* vertex used for N^* exchanges, (d) Feynman diagram for $pd \rightarrow dp$ scattering, (e) Feynman diagram for $pp \rightarrow \pi^+d$ scattering.

there are mainly two types, viz., $J = L + \frac{1}{2}$ (quark-spin doublet), it was already found in SBM that the latter ($J = L - \frac{1}{2}$) make negligible contributions so that these (including their couplings) will henceforth be omitted altogether. Among the $J = L + \frac{1}{2}$ states, the following set will, it is hoped, suffice for the range of energies considered:

$$P_{11}(1470), D_{13}(1520), F_{15}(1690), P'_{11}(1750). \quad (2.8)$$

Of these, P_{11} and P'_{11} are (most probably) radial excitations in an $SU(6) \times O(3)$ classification, while the others represent particles on the main-sequence trajectories. [The omitted N^* states also include the quark-spin quartets whose couplings are intrinsically much lower than those of the quark-spin doublets. These particles are, e.g., $D_{15}(1670)$ and $D'_{13}(1675)$, whose contributions will be ignored.] The couplings of these resonances, which have been continuously refined over the years,¹⁵⁻¹⁸ have their latest refinements described recently in connection with the process of electroproduction.¹⁸ The relevant coupling structures applicable only to the subset (2.8), viz., quark-spin doublet states of $J = L + \frac{1}{2}$, are as follows (unexplained notations are the same as in SBM):

$$C_N f_L(m^2, M_L^2, k^2) \bar{u}(p) i\gamma_5 \gamma \cdot k q_{\mu_1} \dots q_{\mu_L} u_{\mu_1}^{L+1/2} \dots \mu_L (P) \pi(k), \quad (2.9)$$

where $C_N = \frac{5}{3}$ or $\frac{2}{3}\sqrt{2}$ for even- L (56) or odd- L (70) N^* states, respectively, and

$$q_\mu = \frac{1}{2}(k_\mu - p_\mu),$$

$$f_L(m^2, M_L^2, k^2) = C_L^+ \left(\frac{2M_L \times 1.22}{M_L^2 + m^2 + k^2} \right)^{L+1}, \quad (2.10)$$

where

$$(C_2^+)^2 = (C_0^+)^2 = 1.28(4\pi); \quad (C_1^+)^2 = (C_3^+)^2 = 1.5(4\pi). \quad (2.11)$$

This form factor, which incidentally gives the $NN\pi$ coupling constant G (rather than mass shell for all particles) as $G^2/4\pi = 15.4$, has a built-in prescription for the pion off-shell extension, one which will be relevant to the evaluation of the dNN^* vertex. For the radial excitations P_{11} and P'_{11} we use the same form (2.10) with $L=0$, but with the following reduced value of the reduced coupling constant C_0 in order to reproduce the correct $N\pi$ widths of these particles:

$$\frac{C_0^2}{4\pi} \approx 0.18. \quad (2.12)$$

For completeness we note the main points of difference of this prescription with the one used in SBM, viz.: First, the square of the meson

mass now has a negative sign (for reasons see Ref. 18); second, the pion mass is at the outset considered to be off the mass shell, thus avoiding the use of a Ferrari-Selleri form factor²¹ separately as was done in SBM [the numerical value of $2(M_L m)^{1/2} S_F(J)^{1/4}$ used in Eq. (2.11) of SBM is of course the same as $(2M_L \times 1.22)$ used in (2.10)]; third, the momenta in the coupling structure (2.9) are now taken as $q_\mu = \frac{1}{2}(k_\mu - p_\mu)$ instead of k_μ as in SBM. This modification leaves results unaltered on the mass shells of N and π , but not necessarily off their mass shells. Finally we have now taken the basic pion coupling in a pseudovector form, viz., $i\gamma_5 \gamma \cdot k$ rather than in a pseudoscalar form $(M+m)\gamma_5$ as was done in SBM. (Again this convention changes things only off the mass shell.)

While a prescription for off-shell extension to the baryon masses, viz., $M_L^2 \Rightarrow -P^2 \equiv u$ and $m^2 \Rightarrow -(P-k)^2$ can be formally suggested in Eq. (2.10), we have refrained here, as we did in SBM, from proposing such an extension, in view of the huge extrapolation involved. The effect of this inadequacy in prescription on the evaluation of dNN^* vertices is not easy to determine and we consciously abstain from such an exercise. However, there is at least a possibility of incorporating the effect of an off-shell extension in the nucleon mass at the $NN\pi$ vertex corresponding to the N -exchange amplitude to the $pp - \pi^+d$ process through an empirical Ferrari-Selleri-type correction proposed by Heinz and Ross²² to fit the backward πN scattering data, viz.,

$$\frac{g^2(u)}{4\pi} = \frac{g^2(m^2)}{4\pi} \left[\frac{1-D}{1+(u+m^2)/\beta^2} + D \right]^2, \quad (2.13)$$

where

$$D \approx 0.14, \quad \beta = 0.34 \text{ GeV}, \quad (2.14)$$

and $g(m^2)$ represents the $NN\pi$ coupling constant on the (nucleon) mass shell (with a value of 15.5). We note in passing that this off-shell extension for this nucleon leg in $NN\pi$ coupling is also applicable in principle to the $NN\pi$ vertex (momenta p_2, k, n_1) in the dNN^* coupling [Fig. 1(c)]. However, as will be discussed in Sec. III, the internal nucleon line (n_1) is almost on the mass shell, a result of the Yao approximation,⁹ which is still maintained by the KS modification. Therefore this particular correction to the $NN\pi$ vertex of the dNN^* coupling diagram will henceforth be left out of further consideration.

III. dNN^* COUPLINGS AND THE PERCENTAGES OF VARIOUS N^* STATES

One major point of departure in this paper from the procedure of SBM concerns the mode of

evaluation of the $pd \rightarrow dp$ amplitude via the triangle diagram, which was calculated there in the Yao⁹ approximation. Recently the numerical effect of the Yao approximation was discussed in some detail by KS,¹¹ who also gave a suitably modified prescription for the evaluation of the triangle vertex. These authors pointed out that out of the two 4-momentum integrations over d^4n_1 and d^4p_2 , the Cauchy residue theorem is applicable only to the quantity n_1^2 which has a pole at $n_1^2 = -m^2$; however, as a result of the n_1^2 integration, the region of p_2^2 becomes somewhat narrower, i.e., the limits of the p_2^2 integration are $-\infty \leq -p_2^2$

$\leq m^2 - 2\alpha^2$ rather than $-\infty \leq -p_2^2 \leq \infty$, which the Yao approximation presupposes. This revised range of integration, as was shown in Ref. 11, leads to a considerable change in the numerical value of $pd \rightarrow dp$ amplitude via the triangle diagram.

A. The dNN^* vertices

For the evaluation of the dNN^* vertex we are faced with a similar correction (discussed above) to the Yao approximation since the structure of the triangle involved is identical. To recapitulate the essential steps, the structure of the dNN^* vertex is given by

$$\begin{aligned} \bar{u}_C(p) \bar{\Gamma}_L^\mu(d, P) u_{(\mu)}^{L+(1/2)}(P) &= \frac{3}{(2\pi)^4} \int d^4n_1 \left[\frac{m - i\gamma \cdot n_1}{n_1^2 + m^2 - i\epsilon} i G \gamma_5 u(p) \right]^T C^{-1} \bar{\Gamma}(d, n_1) \frac{m - i\gamma \cdot p_2}{p_2^2 + m^2 - i\epsilon} \\ &\times \frac{1}{k^2 + m_\pi^2 - i\epsilon} C_{Nf_L^+}(M_L^2, m^2, k^2) i \gamma_5 \gamma \cdot k q_{\mu_1} \cdots q_{\mu_L} u_{\mu_1 \cdots \mu_L}^{L+(1/2)}(P) \end{aligned} \quad (3.1)$$

where $u_{(\mu)}^{L+(1/2)}(P)$ represents the generalized Rarita-Schwinger²³ spinor and $\bar{u}_C(p) = -\bar{u}(p) C^{-1}$ is the charge conjugated spinor to $\bar{u}(p)$. (Note that compared to SBM, we have now taken an extended structure for the dNN vertex.) To evaluate the d^4n_1 integration, we convert it into an integration over $d^4\bar{k}$, where

$$2\bar{k}_\mu = (n_1 - p_2)_\mu, \quad (3.2)$$

$$d_\mu = (n_1 + p_2)_\mu$$

$$n_1, p_2 = \frac{1}{2}d \pm \bar{k}, \quad (3.3)$$

and

$$n_1^2 + m^2, p_2^2 + m^2 \simeq |\vec{k}|^2 + \alpha^2 \mp m_d \bar{k}_0, \quad (3.4)$$

$$k^2 + m_\pi^2 = -2mT + m_\pi^2, \quad (3.5)$$

where $T = \text{K.E. of the proton}$, and we have neglected terms of $O(\bar{k}_0^2)$. Then (3.4) shows that the integration over $d(n_1^2)$ is equivalent to that over $-m_d d\bar{k}_0$, while (3.3) shows that $d^4n_1 = d^4\bar{k}$; thus by writing $d^4n_1 \Rightarrow d^4\bar{k}$, we can perform the integration separately over \vec{k} and \bar{k}_0 , of which the latter obeys the residue theorem with poles at

$$\bar{k}_0 = |\vec{k}|^2 \pm \frac{\alpha^2}{m_d}. \quad (3.6)$$

As a result of these integrations, the dNN^* form factor reduces to

$$\begin{aligned} \bar{\Gamma}_L^\mu(d, P) &\simeq \frac{3}{16\pi m} G \gamma_5 (m + \frac{1}{2}i\gamma \cdot d) \frac{4\pi N y}{m} \gamma \cdot \epsilon \frac{m_d - i\gamma \cdot d}{2\sqrt{2} m_d} \\ &\times \left\{ \frac{1}{\beta + \alpha} + \frac{t}{\sqrt{2}(\gamma^2 - \alpha^2)^2} [\alpha^3 + \frac{1}{2}\gamma(\gamma^2 - 3\alpha^2)] \right\} \left(\frac{m - \frac{1}{2}i\gamma \cdot d}{m_\pi^2 - 2mT} \right) C_{Nf_L^+}(m^2, M_L^2, k^2) i \gamma_5 \gamma \cdot k \langle q_{\mu_1} \cdots q_{\mu_L} \rangle_{\text{av}}, \end{aligned} \quad (3.7)$$

where β and γ are the usual Yamaguchi²⁴ parameters, and

$$C(\vec{k}^2) = \frac{1}{\beta^2 + \vec{k}^2} \quad (3.8)$$

$$\bar{T}(\vec{k}^2) = \frac{1}{\vec{k}^2} T(\vec{k}^2), \quad T(\vec{k}^2) = -\frac{t \vec{k}^2}{(\gamma^2 + \vec{k}^2)^2}.$$

The evaluation of $\langle k_\mu \rangle$ over the azimuthal depen-

dence of the k_μ variables is exactly as described in SBM and earlier.¹⁵

B. Percentage of N^* states in the deuteron

The dNN^* vertices so evaluated afford an estimation of the percentage probabilities of various N^* states residing in the deuteron. However, instead of calculating the total percentage probabilities, it is simpler to speak of the probability

density in momentum space, e.g., as a function of the u variable, which in turn can be expressed in terms of the incident proton energy corresponding to a fixed angle of scattering. Further it is more convenient to speak of these N^* densities relative to N , rather than in an absolute fashion. For this purpose we first note that the relativistic dNN^* wave function is obtained by multiplying the corresponding vertex function Γ by the propagators $S_F(N)$ and $S_F(N^*)$ for N and N^* , respectively. However, since one nucleon leg is common to both systems, it is adequate for purposes of evaluating the probability of N^* relative to N inside the deuteron to consider the truncated quantities

$$\psi_N = S_F(N)\Gamma(dNN), \quad (3.9)$$

$$\psi_{N^*} = S_F(N^*)\Gamma(dNN^*), \quad (3.10)$$

so that the relative probability density of N^* versus N is given by

$$R = |\psi_{N^*}|^2/|\psi_N|^2. \quad (3.11)$$

We indicate briefly the calculations of the numerator and denominator of (3.11).

For a general value of $J(L + \frac{1}{2})$ we have

$$\frac{1}{2}i S_F(N^*) = \frac{M_L - i\gamma \cdot P}{M_L^2 - u} \Theta_{(\mu)}^{(\nu)}(L + \frac{1}{2}), \quad (3.12)$$

where $\Theta_{(\mu)}^{(\nu)}(L + \frac{1}{2})$ is the projection operator for a state of $J = L + \frac{1}{2}$ as described by many authors.^{25,14} We shall use the following property of this operator, which is valid when the "mass" of the state is taken as $-P^2 = u$:

$$\sum_{\nu} \Theta_{(\mu)}^{(\nu)} \Theta_{(\nu)}^{(\mu')} = \Theta_{(\mu)}^{(\mu')}. \quad (3.13)$$

Using these results and taking the spin average for N^* , we have

$$\langle |\psi_{N^*}|^2 \rangle_{\text{av}} = \frac{1}{2J+1} \text{Tr} \left[\Gamma_L^{(\mu)}(d, P) \frac{M_L - i\gamma \cdot P}{M_L^2 - u} \Theta_{(\mu')}^{(\mu)}(L + \frac{1}{2}) \right. \\ \left. \times \frac{M_L - i\gamma \cdot P}{M_L^2 - u} \bar{\Gamma}_L^{(\mu')}(d, P) \right], \quad (3.14)$$

where for the dNN^* vertex Eq. (3.7) has been employed. Now the calculation of (3.14), as well as its simplification, are done in a straightforward manner. The numerical values of R of Eq. (3.11), which is clearly a function of the u variable, are listed in Tables I and II for two sets of parameters relevant to the incident proton energies considered for the two processes $pd-dp$ and $pp-\pi^+d$, respectively, in this paper. Then results which also include the relative contributions of N and N^* exchanges in this process are discussed further below in Secs. IV and V.

IV. NUMERICAL RESULTS FOR $pd \rightarrow dp$

The total amplitude for this process consists of the sum of contributions from the N and N^* exchanges according to the list (2.8). The formulas for the amplitude and differential cross section ($d\sigma/d\Omega$) are the same as given by Eqs. (2.22) and (2.27)–(2.29) of SBM, except for the replacement of the vertex function $\Gamma_{L,J}$ of (2.22) by the "corrected" vertex function, Eq. (3.7), of this paper.

In Figs. 2(a)–2(c) we give the results for the $pd-dp$ process for a fairly wide range of kinetic energies of the incident proton. The data are available for two groups of energies: viz, the old data of Coleman *et al.*¹ for the energy range 1.0–1.5 GeV and the more recent data of Igo *et al.*⁵ for much lower energies (300–600 MeV). The relative contributions of the N -exchange and N^* -exchange terms at the higher energies (1.0–1.5 GeV) were discussed fully in SBM and those conclusions continue to hold at the present calculation as well, despite the modifications made here in the dNN^* form factors, while at the lower energies (300–600 MeV) the N -exchange contribution almost entirely accounts for the total amplitude. We discuss further below, in tabular form (instead of in the form of curves as in SBM) contributions of N and N^* exchanges in the energy range of 1.0–1.5 GeV, in relation to the percentage probabilities of these particles. Before doing this, it is tempting to compare the full curves with the experimental data points. Indeed it looks rather gratifying that the

TABLE I. Contributions of N and N^* exchanges to the $pd \rightarrow dp$ differential cross section in the backward direction in the energy range 1.0–1.5 GeV. The bracketed quantities are the corresponding probability densities in percent.

N^* T_p (GeV)	$P_{11}(1470)$ (μb)	$P'_{11}(1750)$ (μb)	$D_{13}(1520)$ (μb)	$D_{15}(1675)$ (μb)	$F_{15}(1688)$ (μb)	Nucleon (μb)
1.5	(11.10)0.82	(4.54)0.47	(3.40)0.41	(2.10)...	(0.72)0.53	1.21
1.3	(8.00)1.92	(3.25)1.03	(2.62)1.02	(1.61)0.02	(0.58)1.09	3.02
1.0	(4.45)5.10	(1.75)2.04	(1.51)2.01	(0.94)0.04	(0.40)2.69	9.03

TABLE II. Relative probability densities p_L (in %) corresponding to N^* states inside the deuteron in the backward direction for such exchanges. Also shown are the relative contributions of N^* exchanges with respect to N exchange (in %) to the differential cross sections, separately for "direct" (C_D) and "exchange" (C_X) terms.

N^* T_p (GeV)	$P_{11}(1470)$			$P'_{11}(1750)$			$D_{13}(1520)$			$D_{15}(1675)$			$F_{15}(1688)$		
	$p_L\%$	$C_D\%$	$C_X\%$	$p_L\%$	$C_D\%$	$C_X\%$	$p_L\%$	$C_D\%$	$C_X\%$	$p_L\%$	$C_D\%$	$C_X\%$	$p_L\%$	$C_D\%$	$C_X\%$
1.5	18.21	44.04	13.92	7.02	30.97	11.36	5.14	20.45	5.68	3.25	1.99	0.85	1.54	42.61	13.07
1.3	15.26	51.39	16.39	6.02	33.05	13.88	4.15	24.72	7.77	2.81	3.06	1.11	0.98	50.84	16.11
1.0	12.39	80.60	24.86	5.21	51.91	21.86	3.50	34.15	11.47	1.51	7.92	2.46	0.73	60.65	22.95

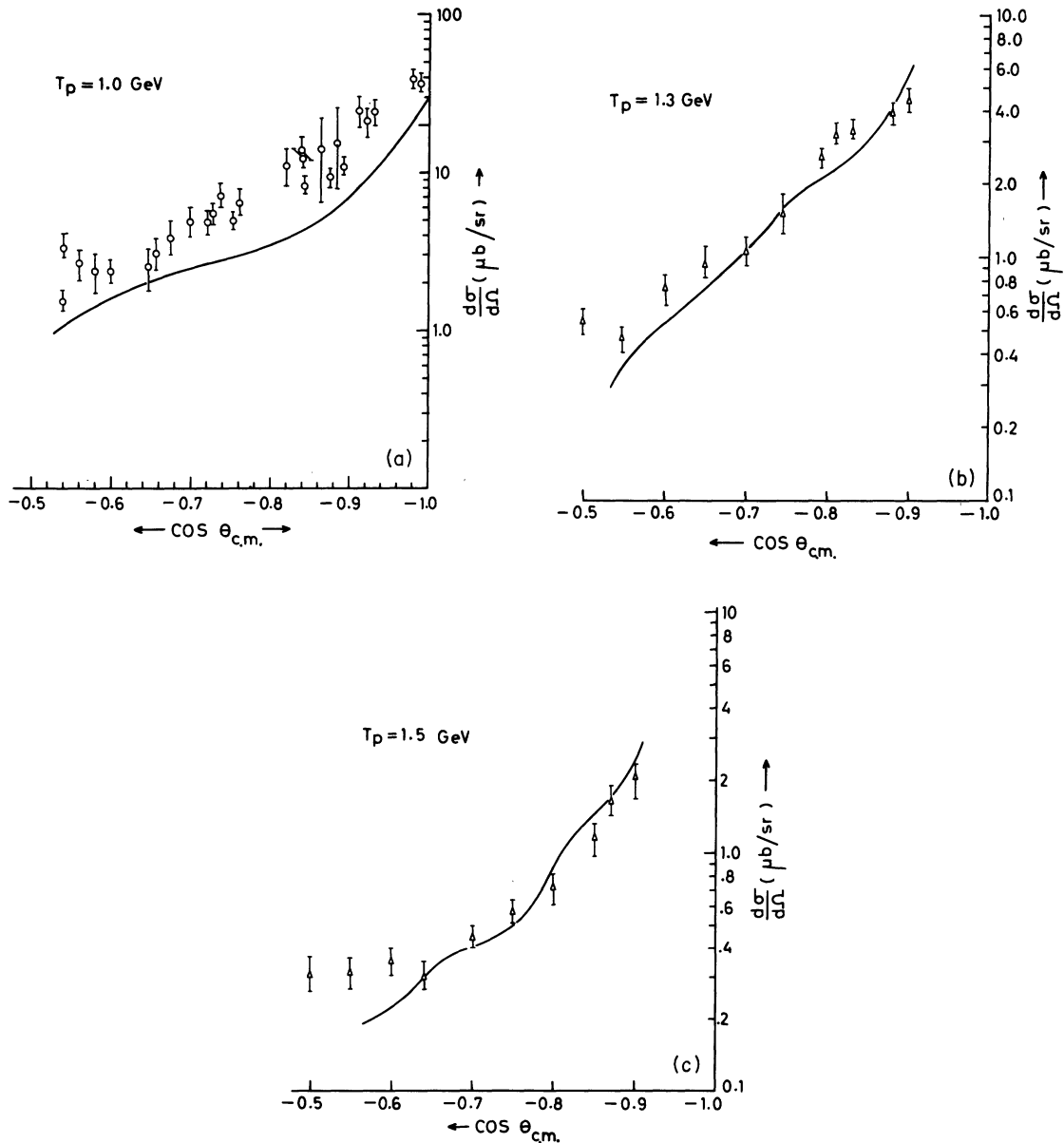


FIG. 2. (a) Differential cross section for $pd \rightarrow dp$ versus θ in the c.m. system for incident (lab) kinetic energies $T_p = 1.0$ GeV. (b) Differential cross section for $pd \rightarrow dp$ versus θ in the c.m. system for incident (lab) kinetic energies $T_p = 1.3$ GeV. (c) Differential cross section for $pd \rightarrow dp$ versus θ in the c.m. system for incident (lab) kinetic energies $T_p = 1.5$ GeV.

fits are quite good for both groups of data at higher and lower energies.

For the higher energies, especially 1.5 GeV, there seems to be a welcome absence of the distortion which had plagued the results of SBM. This is directly attributable to the use of the combination $q_\mu = \frac{1}{2}(k_\mu - p_\mu)$ for the momentum k_μ in the multiple derivative coupling structure (2.9).²⁶ The other modification and correction used, viz. (i) the pseudovector form $(i\gamma_5\gamma^\mu k)$ of $N^*N\pi$ coupling, (ii)

direct off-shell extension in the pion's (mass)² in the modified form factor,¹⁸ (iii) use of the extended dNN vertex throughout, and (iv) the KS correction to the Yao approximation, all seem to have helped to produce rather reasonable magnitudes at all the three energies considered.

For the group of curves corresponding to lower energies (Figs. 3(a)–3(d)) there again seems to be a reasonably good fit to the data, essentially with N exchange, since N^* exchanges just start making

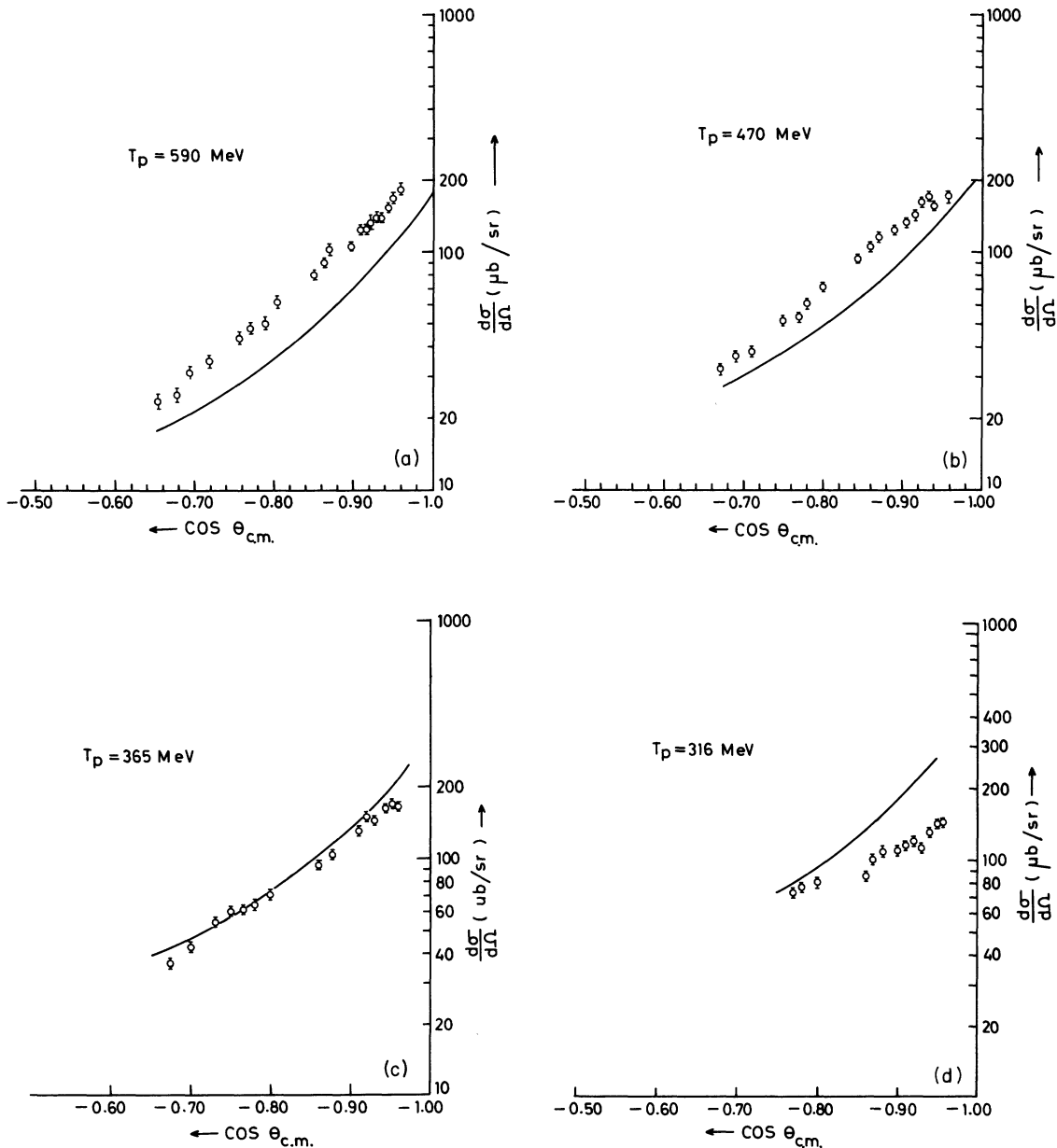


FIG. 3. (a) Same as in Figs. 2(a)–2(c) but for $T_p = 0.590$ GeV. (b) Same as in Figs. 2(a)–2(c) but for $T_p = 0.470$ GeV. (c) Same as in Figs. 2(a)–2(c) but for $T_p = 0.365$ GeV. (d) Same as in Figs. 2(a)–2(c) but for $T_p = 0.316$ GeV.

themselves felt around 600 MeV. The only major source of discrepancy seems to be at 316 MeV, where the theoretical curve is appreciably above the experimental points. We do not completely understand this discrepancy, though we cannot but notice that the trend of data curve in this case is appreciably different from those at other energies, even the one at 365 MeV.²⁷

Table I depicts the individual contributions of the N^* versus N exchanges for the energies 1.0–1.5 GeV. As was found in SBM the collective contribution of the N^* exchanges to the total amplitude far exceeds their individual contributions. Even so, the P_{11} and P'_{11} contributions are comparable to N exchange, thus indicating that, despite their similarity of quantum number to the nucleon, their effect is not quite telescoped in the N -exchange contribution. This (rather unexpected) result must be interpreted to reflect the nontrivial role of the radial structure of the dNP_{11} vertex function from the dNN wave function in this particular model. However, an inspection of Table II shows that the relative probability densities of the P_{11} and P'_{11} to the deuteron are appreciably smaller than that of N , despite their (much larger) relative contributions to $d\sigma/d\Omega$. On the other hand, the contributions of D_{13} and F_{15} are much more modest even at the higher energies. Indeed the percentage figure for F_{15} (viz., 0.72%) does not violate the estimate of KK, though the roles of P_{11} and P'_{11} have no counterparts in their model. (Note, however, that our calculations of probability densities at a given angle cannot be directly compared with the evaluation of integrated probabilities such as was done by KK.)

Finally we give in Fig. 4 a plot of energy variation of $d\sigma/d\Omega$ at $\cos\theta_{c.m.} = -0.96$ (almost backward direction). The general trend which is in reasonable agreement with experiment seems to indicate a sharp fall with energy, a feature which had also been predicted by CW on the basis of their triangle (π -exchange) mechanism.²⁸ Again the role of N^* exchange is crucial, since without this contribution the fall would have been far more precipitous, in disagreement with experiment.

V. THE CROSS SECTION AND NUMERICAL RESULTS FOR $pp \rightarrow \pi^+ d$

In this section we consider the related process $p\bar{p} \rightarrow \pi^+ d$ for which we give some essential details, as this process was not considered in SBM. This process has already been investigated theoretically^{9,29} and experimentally^{3,7,8} by some authors, but the theoretical calculations are not sufficient to reproduce the desired experimental features.

A. The cross section

The 4-momenta of the particles involved are as shown in Fig. 1(e), viz., $\hat{p}'_\mu, \hat{p}_\mu$ of two initial-state protons and \hat{k}_μ, \hat{d}_μ of final-state meson and deuteron, respectively. The only additional feature of this process (not shared by $p\bar{d} \rightarrow d\bar{p}$) is the role of Fermi statistics for the initial $p\bar{p}$ state. The simplest way to incorporate this effect is to follow Yao⁹ in writing the total invariant amplitude as

$$A(p, p') = T(p, p') - T(p', p), \quad (5.1)$$

where the first term on the right-hand side represents the amplitude corresponding to Fig. 1 and is expressed by

$$T(p, p') = T_N(p, p') + \sum_{N^*} T_{N^*}(p, p'). \quad (5.2)$$

Note that the term $T(p', p)$ can be obtained simply by interchanging the two initial-state protons. Here in Eq. (5.2) T_N and T_{N^*} are the contributions to the amplitude (unsymmetric) due to N and N^* exchanges, respectively. Thus

$$T_N = \bar{u}_C(p) \bar{\Gamma}(d, p) \frac{m - \hat{\gamma} \cdot \hat{p}}{m^2 - u} \sqrt{2} \gamma_5 g(u) u(p'), \quad (5.3)$$

where we now have Eqs. (2.1) and (2.13) for the dNN and $NN\pi$ vertices, respectively. Similarly T_{N^*} can be expressed

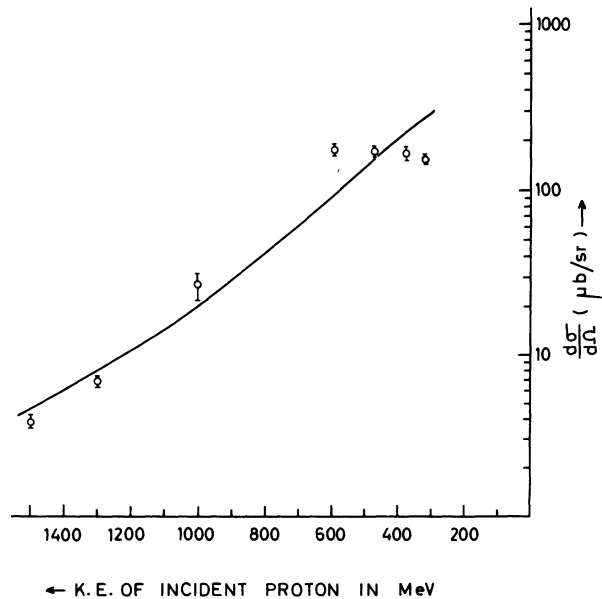


FIG. 4. Energy distribution of backward ($\theta \approx \pi$) cross section for $p\bar{d} \rightarrow d\bar{p}$.

$$\sum_{N^*} T_{N^*} = \sum_L \bar{u}_C(\not{p}) \bar{\Gamma}_L^{(\mu)}(d, P) \frac{1}{2} i S_F^{(\mu, \nu)}(P, M_L) \times \sqrt{2} V_L^{(\nu)}(p', k) u(p'), \quad (5.4)$$

where $\Gamma_L^{(\mu)}(d, p)$ (dNN^* vertex) is given by Eq. (3.7) and V_L consists of the following factor of Eq. (2.9):

$$V_L^{(\nu)}(p', k) = C_{N^*} f_L(m^2, M_L^2, k^2) i \gamma_5 \gamma^\nu k q'_{\mu_1} \dots q'_{\mu_L}, \quad q'_\mu = \frac{1}{2}(p' - k)_\mu. \quad (5.5)$$

Finally the cross section for $pp \rightarrow \pi^+ d$ is given in terms of the antisymmetric amplitude (5.1) as

$$\left(\frac{d\sigma}{d\Omega_d} \right) = \frac{1}{16\pi^2} m^2 \left(\frac{2m_d}{s} \right) \left(\frac{p_C^f}{p_C^i} \right) \left(\frac{1}{4} \sum_{\text{spins}} |A|^2 \right), \quad (5.6)$$

where $s = -(p + p')^2$ and $p_C^{i,f}$ are the initial (final) c.m. 3-momenta, respectively. Because of the obvious symmetry of $|A|^2$ with respect to $\Theta_d = 90^\circ$, for this process the cross section could have been equally well expressed as a function of $(\pi - \Theta_d)$ as pointed out, e.g., by Brown,²⁹ but it is adequate to consider the cross section corresponding to the backward direction of the deuteron around which the data are available.³

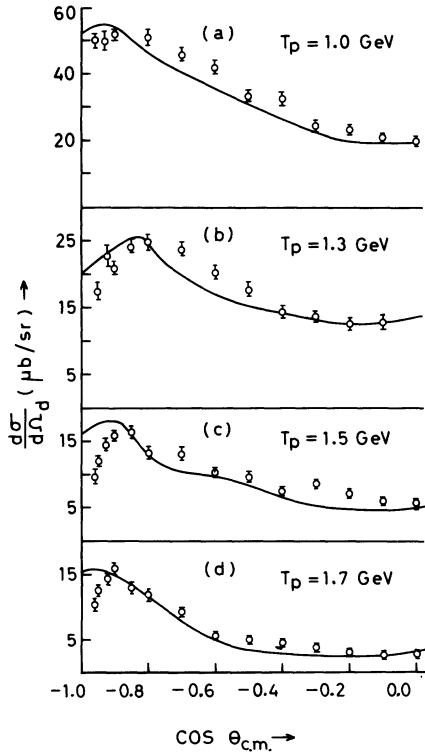


FIG. 5. Differential cross section for $pp \rightarrow \pi^+ d$ versus θ in the c.m. system for the incident (lab) kinetic energies $T_p = 1.0, 1.3, 1.5,$ and 1.7 GeV.

B. Numerical results

In this subsection we shall describe the quantitative and qualitative nature of our results obtained by the model of N and N^* exchanges in relation to the experimental data. The differential cross section in the c.m. system has been calculated by Eq. (5.6) for the incident proton kinetic energies $T_p = (0-2.8$ GeV) and is represented in Figs. 5 and 6 with the corresponding experimental data.³

As in the case of $pd \rightarrow dp$, the main contributors (apart from N exchange) are the $N^*(J = L + \frac{1}{2})$ exchanges, $P_{11}(1470)$, $P'_{11}(1750)$, $D_{13}(1520)$, and $F_{15}(1690)$, while $J = L - \frac{1}{2}$ exchanges play, at most, a nominal role. The calculated curves, according to Eq. (5.6), seem to reproduce the data in sufficient details, except for the fact that the humps near the backward direction which characterize the energies below 2.0 GeV are much sharper than the calculated ones. In effecting this agreement the N^* exchanges have played a twofold role: (i) enhancing the cross section by 20% to 25%, and more important, (ii) improving the shape of the angular distribution compared to the mere N exchange term. The antisymmetrization in the initial pp state, which produces an enhancement of about 30% as a result of interference between "direct" and "exchange" terms as in the right-hand side of Eq. (5.1), helps in producing the bend-over of $d\sigma/d\Omega$ near $\theta = \pi$ for $E < 2.0$ GeV. Inclusion of N^* exchanges further helps to sharpen the bend-

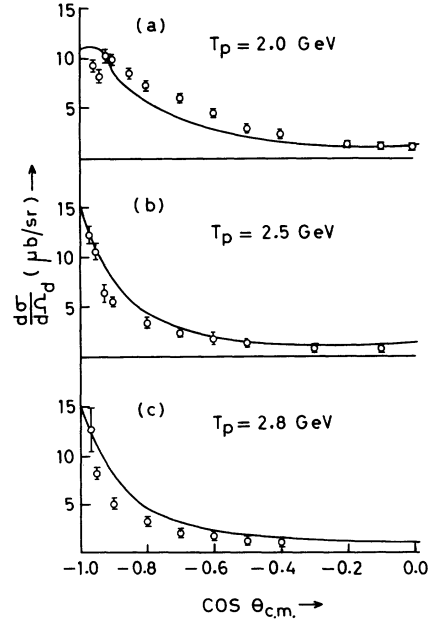


FIG. 6. Same as in Fig. 5 but for $T_p = 2.0, 2.5,$ and 2.8 GeV.

over somewhat, though it still appears to fall short of the experimental requirement.

Another comparison of interest is the energy variation at backward angles with the data. For this purpose we have plotted in Fig. 7 appropriate experimental points (i.e., in the backward direction) extracted from the angular distribution curves of Heinz *et al.*³ at different values of the energy. The general fit seems to be rather good, in marked contrast to the results of N exchange or pion-exchange¹⁰ (triangle) models,³⁰ in terms of both the absolute magnitude as well as the shape.

There are, however, some fluctuations around 2 GeV which we do not quite understand. If this discrepancy is to be taken seriously, one might speculate on the (s -channel) effect of some $Y=B=2$ resonance, about which there has been some discussion in recent experimental literature.³⁰⁻³⁴ Such a state, which was first suggested by Dyson³⁵ as a ΔN bound state (or resonance), could also be regarded as a Regge recurrence of the singlet deuteron.³⁴ However, the discrepancy between the data and the theoretical curves is not strong enough to make such an inference in any causal manner.

VI. SUMMARY AND CONCLUSION

In this paper we have tried to present a unified account of the two related processes $pd-dp$ and $pp-\pi^+d$ within the framework of a scheme of higher baryon couplings developed by this group in recent years, along the lines of the general KK idea of the importance of resonance exchanges for such processes in the medium and intermediate energy region, but with considerable departures in details. In a way the work presented here is an extension of our earlier work on $pd-dp$ to include a much wider range of energies than was possible in SBM. However, we have taken the opportunity to effect several improvements (in details) on our earlier approach, and also included a parallel description of the allied process $pp-\pi^+d$ for the sake of completeness. The improvements include (i) use of the extended dNN vertex throughout, (ii) replacement of the "pseudoscalar" form $(M+m)\gamma_5$ of $NN\pi$ (or $NN\pi^*$) coupling by the "pseudovector" form $i\gamma \cdot k\gamma_5$, (iii) the replacement of k_μ by the Blankenbecler and Sugar³⁶ antisymmetrized combi-

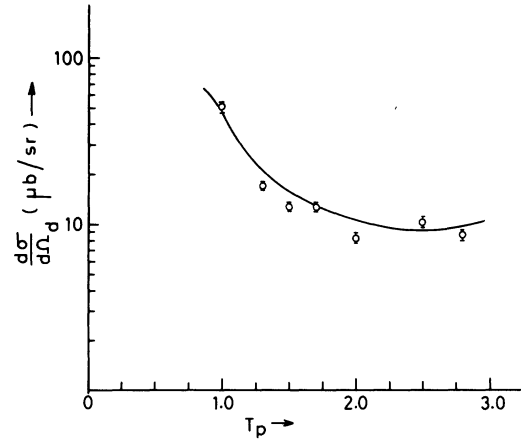


FIG. 7. Energy distribution of backward ($\theta \approx \pi$) cross section for $pp \rightarrow \pi^+d$.

nation $q_\mu = \frac{1}{2}(k_\mu - p_\mu)$, and (iv) the KS correction to the Yao approximation. For the $pd-dp$ case, the fits are now good over an entire energy range of 360 to 1.5 GeV without the angular distortions for higher energies noticed in SBM. A similar degree of success is also noticeable in the $pp-\pi^+d$ case for the energy range 1.0–2.8 GeV, with identical assumption on the N - and N^* -exchange vertices.

The model has one unpleasant feature: It predicts a surprisingly large contribution (*a priori*) arising from the P_{11} and P'_{11} , particularly the former, the only redeeming feature in this respect being that the percentage probabilities of these states inside the deuteron are much less pronounced than their contributions to the cross section. On the other hand, the contributions of D_{13} and F_{15} to $d\sigma/d\Omega$ as well as their percentage probabilities in the deuteron are far more modest. This study still leaves unanswered many questions, such as the roles of still higher resonances and the behavior of these processes at still higher energies.

ACKNOWLEDGMENTS

One of us (JSS) acknowledges a Council of Scientific and Industrial Research (India) fellowship. The other (ANM) recalls with pleasure a stimulating conversation with B.S. Bhakar and V. S. Bhasin on the role of a possible ΔN resonance in such processes.

¹E. Coleman *et al.*, Phys. Rev. Lett. **16**, 761 (1966).

²G. Bennett *et al.*, Phys. Rev. Lett. **19**, 387 (1967).

³R. M. Heinz *et al.*, Phys. Rev. **167**, 1232 (1968).

⁴R. M. Heinz, Ph.D. thesis, Univ. of Michigan, 1964

(unpublished).

⁵G. Igo *et al.*, National Bureau of Standards report, 1971 (unpublished).

⁶D. Dekkers *et al.*, Phys. Lett. **11**, 161 (1964).

- ⁷F. Turkot *et al.*, Phys. Rev. Lett. 11, 474 (1963).
- ⁸H. L. Anderson *et al.*, Phys. Rev. D 3, 1536 (1971).
- ⁹T. Yao, Phys. Rev. 134, B454 (1964).
- ¹⁰N. S. Craigie and C. Wilkin, Nucl. Phys. 14B, 477 (1969) (hereafter referred to as CW.)
- ¹¹V. M. Kolybasov and Smorodinskaya, Phys. Lett. 37B, 272 (1971) (hereafter referred to as KS).
- ¹²A. Kerman and L. Kisslinger, Phys. Rev. 180, 1483 (1969) (hereafter referred to as KK).
- ¹³L. Bertocchi and A. Capella, Nuovo Cimento 49, 206 (1967).
- ¹⁴J. S. Sharma, V. S. Bhasin, and A. N. Mitra, Nucl. Phys. 35B, 466 (1971) (hereafter referred to as SBM).
- ¹⁵A. N. Mitra, Ann. Phys. 67, 518 (1971).
- ¹⁶D. K. Choudhury *et al.*, Nuovo Cimento Lett. 2, 265 (1971).
- ¹⁷R. Mehrotra *et al.*, Phys. Rev. D 5, 1803 (1972); S. A. S. Ahmed *et al.*, *ibid.* 7, 2125 (1973).
- ¹⁸Sudhir K. Sood and A. N. Mitra, Phys. Rev. D 7, 2111 (1973).
- ¹⁹M. Gourdin *et al.*, Nuovo Cimento 37, 524 (1965).
- ²⁰R. Blankenbecler *et al.*, Nucl. Phys. 12, 629 (1959).
- ²¹E. Ferrari and F. Selleri, Nuovo Cimento Suppl. 24, 453 (1962).
- ²²R. M. Heinz and M. H. Ross, Phys. Rev. Lett. 14, 1091 (1965).
- ²³C. Fronsdal, Nuovo Cimento Suppl. 2, 416 (1958).
- ²⁴Y. Yamaguchi and Y. Yamaguchi, Phys. Rev. 95, 1635 (1954).
- ²⁵Adapted from J. C. Taylor, Oxford report, 1968 (unpublished).
- ²⁶Actually there is a tendency for cancellation between the D_{13} and F_{15} contributions, for each of which the effect of antisymmetrization is still larger, yet the net effect is not to be considered insignificant.
- ²⁷One possibility that comes to our mind lies in the role of the hard core in deuteron structure—an effect we have not considered in this paper. But then it is difficult to understand why the agreement should be so good at the next higher energy of 365 MeV.
- ²⁸The structure around 400–600 MeV (Fig. 9), which is not reproduced in this simple model of N and N^* exchanges, is probably due to the (neglected) effect of the 33 resonance, which must be considered through more complicated diagrams since a deuteron can accommodate the 33 resonance only in a pair. For the importance of this state in the deuteron, see, e.g., N. R. Nath, H. J. Weber, and P. K. Kabir, Phys. Rev. Lett. 26, 1404 (1971).
- ²⁹D. J. Brown, Nucl. Phys. 7B, 37 (1968); D. J. Brown and M. K. Sundaresan, Nuovo Cimento 55A, 346 (1968).
- ³⁰R. Yazykarneev and A. M. Rozanova, Zh. Eksp. Teor. Fiz. 59, 1444 (1970) [Sov. Phys.—JETP 32, 788 (1971)].
- ³¹L. S. Schroeder *et al.*, Phys. Rev. Lett. 27, 1813 (1971).
- ³²B. S. Bhakar and V. S. Bhasin, in *Proceedings of the International Conference on Few Particle Problems in Nuclear Physics, Los Angeles, California, 1972*, edited by I. Šlaus, S. A. Moszkowski, R. P. Haddock, and W. T. H. van Oers (North-Holland, Amsterdam, 1973).
- ³³C. W. Akerlof, R. E. Hicker, A. D. Krisch, K. W. Edwards, L. G. Ratner, and K. Ruddik, Phys. Rev. 159, 1138 (1967).
- ³⁴D. Bessis *et al.*, Phys. Rev. D 1, 2064 (1970).
- ³⁵F. J. Dyson *et al.*, Phys. Rev. Lett. 13, 815 (1964).
- ³⁶R. Blankenbecler and R. Sugar, Phys. Rev. 168, 1597 (1968).